

Journal of
Mechanics of
Materials and Structures

**NEW CONCEPTION OF THE FEM BASE FUNCTIONS APPLIED TO
SOLVING AN INVERSE HEAT TRANSFER PROBLEM**

Andrzej Frąckowiak, Jens von Wolfersdorf and Michał Ciałkowski

Volume 3, N° 6

June 2008



mathematical sciences publishers

NEW CONCEPTION OF THE FEM BASE FUNCTIONS APPLIED TO SOLVING AN INVERSE HEAT TRANSFER PROBLEM

ANDRZEJ FRĄCKOWIAK, JENS VON WOLFERSDORF AND MICHAŁ CIAŁKOWSKI

The present work shows the modified concept of the finite element method which has been applied to the solution of the inverse problem (of Cauchy type) for heat conduction equation in a circular ring. The main idea of the new concept consists of the application a new type of base function which cause the vanishing of some integrals in the strong formulation. The calculation with the new base functions takes place in the physical space, and there is no need to go to the isoparametric one. Numerical calculations of the inverse problem confirm the good properties of a new set of base functions.

1. Introduction

The complex character of the domain and the equations depicting heat-flow problems in arbitrary bodies impose the need for use of numerical methods such as the finite element method (FEM) for solving them. In order to satisfy continuity of a function between particular finite elements isoparametric elements are typically used, which, in consequence, results in increased computational costs. In order to reduce the computational effort and satisfy continuity of the interpolated function in the entire domain at the same time, interpolation of the solution at the element (the physical space) is proposed with the use of a new type of base functions.

Consideration of the heat conduction equation in discretized form is conducive to some integrals that should be numerically calculated. In order to avoid some of the integrals, test functions are introduced. Their regularity affects accuracy of the temperature field computed this way.

The method proposed in the present paper is a generalization of the finite element methods presented in [Gresho and Sani 2000]. Aspects of such an approach are discussed below.

2. Numerical method for solving the direct and inverse problems

In order to present the new conception let us consider the Laplace equation in the Ω domain, as shown in Figure 1:

$$\Delta T = 0, \quad T \in C^2(\Omega_i). \quad (2-1)$$

First, the neighborhood of the point P_i is considered. The elements including the point P_i form the domain

$$\Omega_i = \bigcup_{\alpha=1}^{n_i} \Omega_{i\alpha}.$$

Keywords: inverse problem, finite element method.

This paper was done with support from a grant from the Ministry of Higher Education (no. 3134/B/T02/2007/33).

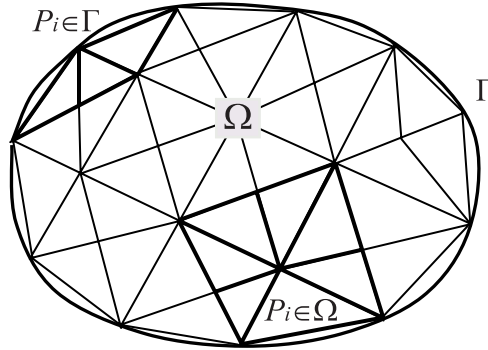


Figure 1. The domain Ω divided into elements.

Let the test function $w \in C^2(\Omega_{i\alpha}) \cap C^1(\Omega_i)$. Multiplication of Equation (2-1) by the w function and integration over the Ω_i domain provides

$$\int_{\Omega_i} \Delta T \cdot w \cdot d\omega = \sum_{\alpha=1}^{n_i} \int_{\Omega_{i\alpha}} \Delta T \cdot w \cdot d\omega = \sum_{\alpha=1}^{n_i} \int_{\partial\Omega_{i\alpha}} [\text{div}(\nabla T \cdot w) - \text{div}(T \cdot \nabla w)] \cdot d\omega + \sum_{\alpha=1}^{n_i} \int_{\Omega_{i\alpha}} T \cdot \Delta w \cdot d\omega = 0.$$

Application of the Gauss–Ostrogradski theorem gives

$$\sum_{\alpha=1}^{n_i} \int_{\partial\Omega_{i\alpha}} \left(w \cdot \frac{\partial T}{\partial n} - T \cdot \frac{\partial w}{\partial n} \right) \cdot ds + \sum_{\alpha=1}^{n_i} \int_{\Omega_{i\alpha}} T \cdot \Delta w \cdot d\omega = 0, \quad i = 1, 2, \dots \tag{2-2}$$

Taking into account continuity of the w function within the element Ω_i and continuity of the derivative $\partial T/\partial n$, the integral of the product $w \cdot \partial T/\partial n$ at common boundaries $\partial\Omega_{i\alpha}$ between the elements vanishes, so that

$$\sum_{\alpha=1}^{n_i} \int_{\partial\Omega_{i\alpha}} w \cdot \frac{\partial T}{\partial n} \cdot ds = \int_{\partial\Omega_i} w \cdot \frac{\partial T}{\partial n} \cdot ds. \tag{2-3}$$

The integral at the right-hand side of Equation (2-3) disappears provided that $w|_{\partial\Omega_i} = 0$. The essence of the present conception consists of the formulation of such a test function that takes zero values at the $\partial\Omega_i$ boundary. In consequence, the number of integrals of (2-2) is reduced. Moreover, if the w function is differentiable in the domain Ω_i , the first sum of (2-2) disappears too. Let us consider the case $w \in C^2(\Omega_{i\alpha}) \cap C^1(\Omega_i) \cap C^0(\partial\Omega_i)$. There, with (2-2), the point $P_i \notin \Gamma$, shown in Figure 2a, takes the form

$$-\sum_{\alpha=1}^{n_i} \int_{\partial\Omega_{i\alpha}} T \cdot \frac{\partial w}{\partial n} \cdot ds + \sum_{\alpha=1}^{n_i} \int_{\Omega_{i\alpha}} T \cdot \Delta w \cdot d\omega = 0, \quad i = 1, 2, \dots \tag{2-4}$$

The condition $P_i \in \Gamma$, shown in Figure 2b, results in $w = 0$ at the boundary $\partial\Omega_i \setminus \Gamma \in \Omega_i$. This gives, for (2-2), the form

$$\int_{\Gamma_i} w \cdot \frac{\partial T}{\partial n} \cdot ds - \sum_{\alpha=1}^{n_i} \int_{\partial\Omega_{i\alpha}} T \cdot \frac{\partial w}{\partial n} \cdot ds + \sum_{\alpha=1}^{n_i} \int_{\Omega_{i\alpha}} T \cdot \Delta w \cdot d\omega = 0, \quad i = 1, 2, \dots \tag{2-5}$$

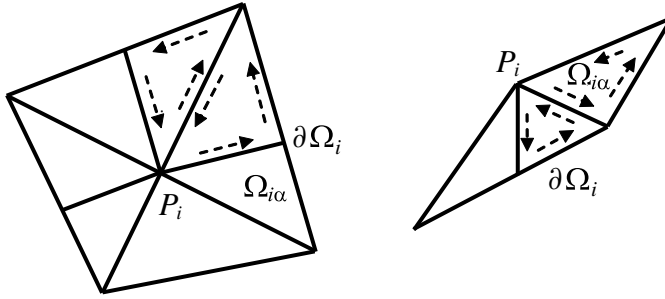


Figure 2. Neighbourhood Ω_i of the P_i points inside (left) and outside (right) of the mesh.

The above equations form a basis for solving the stationary equation of heat conduction with FEM. An important feature of this approach is that only an approximation of temperature function T in the $\Omega_{i\alpha}$ domain is sufficient for solving the equation, without differentiation of the T function approximation or other operations performed on derivatives of the function. The normal derivative of the T function at the boundary of the Ω domain is considered as an independent variable and determined from the boundary conditions. The solution of the Laplace equation in the $\Omega_{i\alpha}$ element is approximated by the function

$$T(P) = \sum_{i=1}^m T_i \cdot \varphi_{i\alpha}(P), \tag{2-6}$$

where the base functions $\varphi_{i\alpha}$ meet the condition

$$\varphi_{i\alpha}(P_j) = \begin{cases} 1, & i = j, \\ 0, & i \neq j. \end{cases} \tag{2-7}$$

The base functions $\varphi_{i\alpha}$ are formulated on the grounds of the observation that

$$\varphi_{PL}(x, y) = \frac{A_L x + B_L y + C_L}{A_L x_p + B_L y_p + C_L}, \tag{2-8}$$

where $A_L x + B_L y + C_L = 0$ is the equation of the straight line L and (x_p, y_p) are the coordinates of the point P (shown in Figure 3), satisfying the condition (2-7) and taking zero values at the line L .

The base functions $\varphi_{i\alpha}$ are products of the functions for various straight lines, (2-8), and the same point P ,

$$\varphi_{i\alpha}(x, y) = \varphi_{ij_1}(x, y) \cdot \varphi_{ij_2}(x, y), \tag{2-9}$$

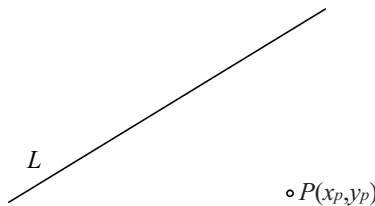


Figure 3. Element line and point for base function considerations.

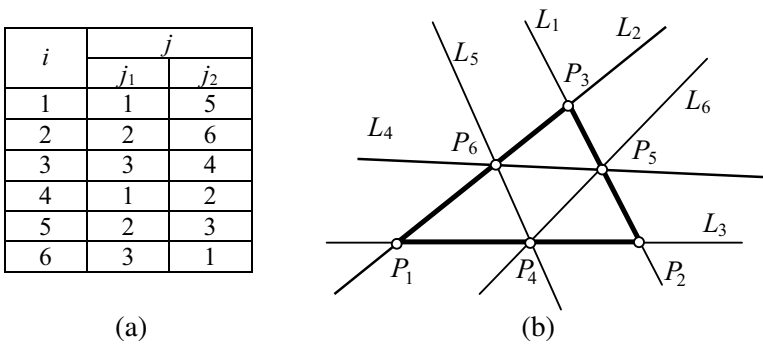


Figure 4. Relationships for base functions.

where the index i is related to the point P , while the indices j_1 and j_2 are related to the straight lines L .

Consideration of the 6-node triangular element of the mesh as shown in Figure 4b enables us to formulate the base function $\varphi_{i\alpha}$ given by Equation (2-9) for each of the nodes $P_i, i = 1, 2, \dots, 6$, where the indices j_1 and j_2 related to the straight lines L are defined in Figure 4. More universal formulation of this type of base functions is described in [Frąckowiak ≥ 2008].

The function $\varphi_{i\alpha}$ defined by (2-9) in the domain $\Omega_{i\alpha}$, apart from having the property (2-7), takes zero values at the sides of the mesh element including no point P . Based on this function let us define another function $\varphi_i(Q)$ continuous in $\Omega_i, \varphi_i(Q) = \varphi_{i\alpha}(Q)$, with $Q \in \Omega_{i\alpha}$ and $\alpha = 1, 2, \dots, n_i$. This definition gives evidence that the function $\varphi_i(Q)$ takes zero values at the boundary $\partial\Omega_i$ of the Ω_i element that bounds the neighborhood of the inner point P_i . When the point P_i is located at the outer boundary Γ , the $\varphi_i(Q)$ function is nonzero at the part of the boundary $\Gamma \cap \partial\Omega_i$.

The above property and the assumption of continuity of the function $\varphi_i(Q)$ in Ω_i provide a basis for solving the problem with FEM.

Substitution of an approximate solution (2-6) into (2-4) and (2-5) and the use of a linear approximation of the normal derivative between the nodes of the Γ boundary allow us to formulate a system of equations in the matrix form

$$\begin{aligned} A_{\Omega\Gamma} T_\Gamma + A_{\Omega\Omega} T_\Omega &= O, \\ A_{\Gamma\Gamma} T_\Gamma + A_{\Gamma\Omega} T_\Omega &= B_\Gamma Q_\Gamma. \end{aligned} \tag{2-10}$$

The number of nodes of the entire field is n . There are inner n_Ω and boundary n_Γ ($n = n_\Gamma + n_\Omega$) nodes. Determining the vector T_Ω from the first equation of (2-10), $T_\Omega = -A_{\Omega\Omega}^{-1} A_{\Omega\Gamma} T_\Gamma$, and substituting into the other, we obtain $(A_{\Gamma\Gamma} - A_{\Gamma\Omega} A_{\Omega\Omega}^{-1} A_{\Omega\Gamma}) T_\Gamma = B_\Gamma Q_\Gamma$. This expression is a relationship well known in the boundary element method,

$$AT_\Gamma = B_\Gamma Q_\Gamma. \tag{2-11}$$

3. Analytical solution of the inverse problem of heat conduction

The application of the new type of base functions will be illustrated using an analytical solution of an inverse problem for a circular ring (see Figure 5).

The ring has an outer radius $r_o = 1$ and an inner radius $r_i < r_o$. The inverse heat conduction problem may be formulated in dimensionless coordinates by giving the distributions of temperature and heat flow

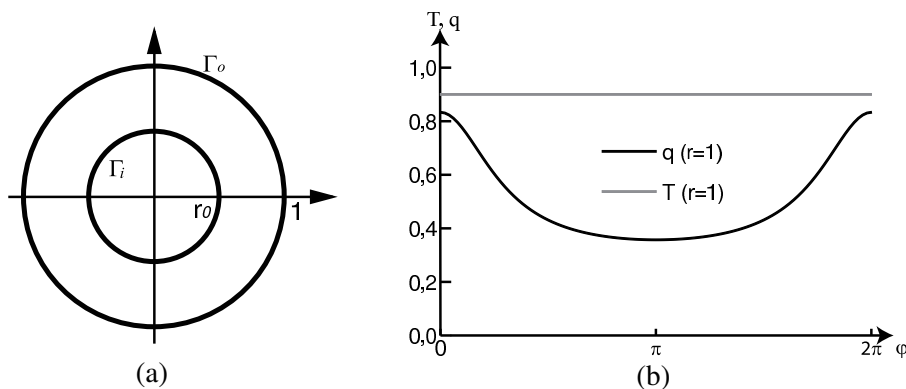


Figure 5. Temperature and heat flow density distributions at the outer boundary of the ring $C = 0.5, a = 0.4, T_c = 0.9, r_i = 0.5$.

density at the outer boundary of the ring [Wróblewska et al. 2008].

$$\Gamma_o : T_{wo} = T_c, \quad q_o = C \cdot \frac{1 - a \cos \varphi}{(1 + a^2 - 2a \cos \varphi)}, \quad a \leq r_i.$$

Moreover, the temperatures in the neighborhoods of the outer and inner boundaries, $T_o = 1$ and $T_i = 0$, are known. The objective is to determine the heat flow and temperature distributions at the inner surface of the ring.

Solution of such a problem is achieved by power series expansion of the q_o function determined at the outer ring boundary,

$$\begin{aligned} q_o &= C \cdot \frac{1 - a \cos \varphi}{(1 + a^2 - 2a \cos \varphi)} = C \cdot \operatorname{Re} \left(\frac{1}{1 - a e^{i\varphi}} \right) \\ &= C \cdot \operatorname{Re} \left(\sum_{m=0}^{\infty} (a \cdot e^{i\varphi})^m \right) = C \cdot \sum_{m=0}^{\infty} a^m \cos(m\varphi), \end{aligned}$$

and hence

$$T(r, \varphi) = T_c + C \cdot \ln(r) + C \cdot \sum_{m=1}^{\infty} \frac{1}{2m} \left[(ar)^m - \left(\frac{a}{r} \right)^m \right] \cos(m\varphi). \tag{3-1}$$

Based on the solution of the inverse problem (3-1) the temperature and heat flow density patterns at the outer boundary (see Figure 5) are determined, for which the inverse problem is to be solved. For the given temperatures outside T_o and inside T_i the ring distributions of normalized heat transfer coefficients with regard to the angle,

$$\Gamma_o : \alpha_o = \frac{q_o}{(T_o - T_{wo})}, \quad \Gamma_i : \alpha_i = \frac{q_i}{(T_i - T_{wi})},$$

are shown in Figure 6.

The vectors of temperatures and heat flow at the ring domain boundary, T_Γ and Q_Γ , that appear in the formula (2-11) are decomposed into the values related to the outer and inner ring boundaries, respectively,

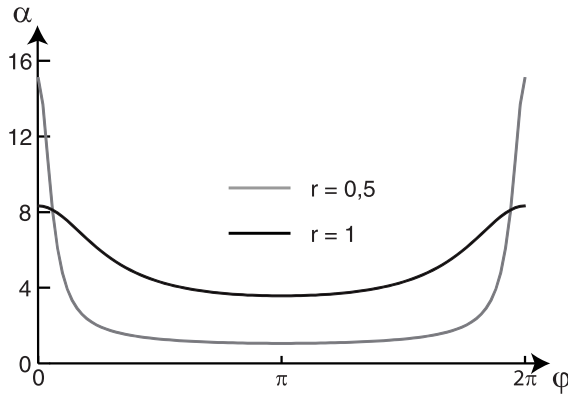


Figure 6. Distributions of heat transfer coefficients α at the inside and outside ring boundaries $C = 0.5, a = 0.4, T_c = 0.9, r_i = 0.5$.

as

$$T_\Gamma = \begin{bmatrix} T_{wo} \\ T_{wi} \end{bmatrix}, \quad Q_\Gamma = \begin{bmatrix} q_o \\ q_i \end{bmatrix}.$$

The relationship (2-11) is then transformed to obtain a solution of the inverse problem [Frąckowiak et al. 2006],

$$\begin{bmatrix} T_{wi} \\ q_i \end{bmatrix} = [-B_i \ A_i]^T [B_o \ -A_o] \begin{bmatrix} T_{wo} \\ q_o \end{bmatrix}. \tag{3-2}$$

This relationship may also be so transformed as to consider the third kind of boundary condition of the direct problem [Frąckowiak et al. 2006]

$$\begin{bmatrix} T_{wo} \\ T_{wi} \end{bmatrix} = [B_o + \alpha_o A_o \ B_i + \alpha_i A_i]^{-1} [\alpha_o A_o \ \alpha_i A_i] \begin{bmatrix} T_o \\ T_i \end{bmatrix}.$$

4. Results of the numerical calculation

The ring, shown in Figure 5, is divided into 450 triangular domains, see Figure 7, thus generating 200 points located at the ring boundary (100 at the inner one and 100 at the outer) and 700 inner points. The direct and inverse problems of ring cooling have been solved according to the method proposed in the present paper.

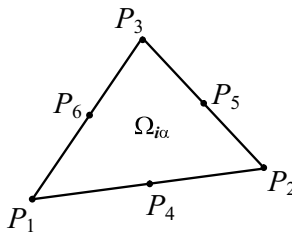


Figure 7. A mesh element.

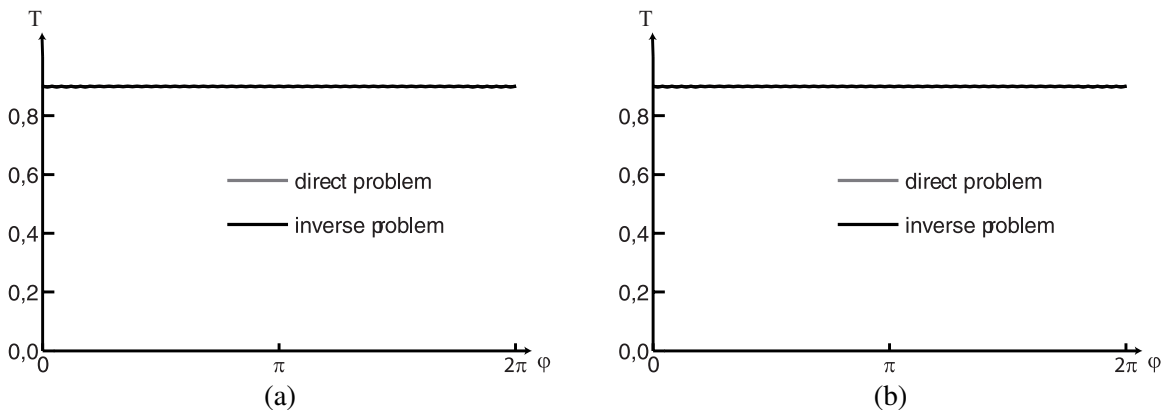


Figure 8. Temperature distribution at the outer (a) and inner (b) boundaries for the direct and inverse problems.

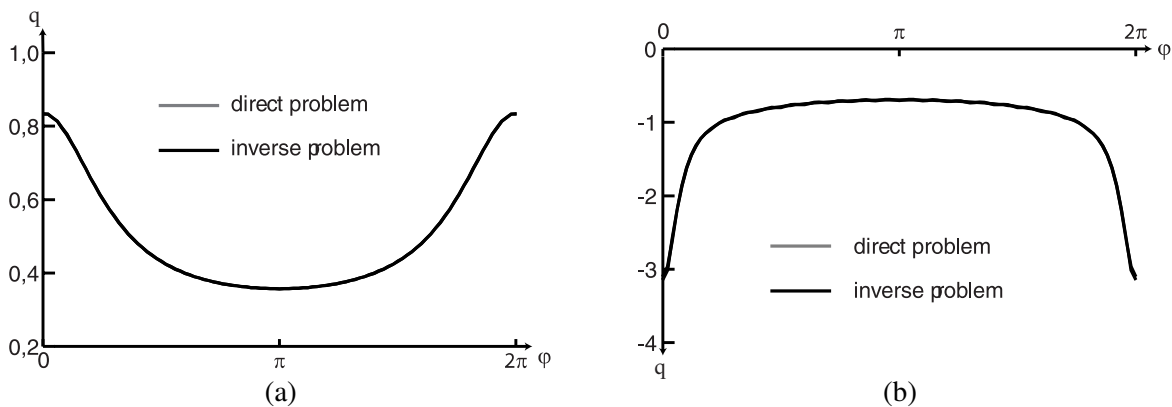


Figure 9. Heat flow density distribution at the outer (a) and inner (b) boundaries for the direct and inverse problems.

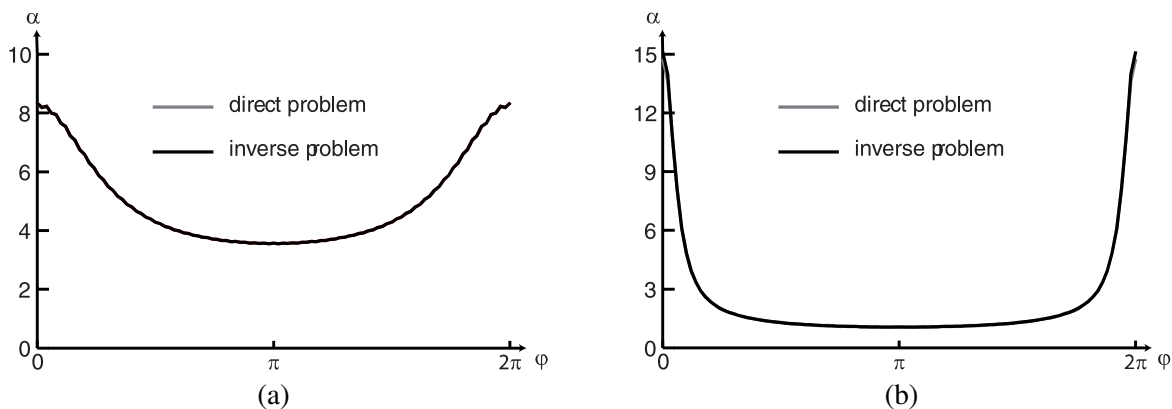


Figure 10. Normalized heat transfer coefficient α distributions at the outer (a) and inner (b) boundaries for the direct and inverse problems.

Type			Temperature error δL_{2T} [%]					
	m	f	$\epsilon_{max}=0$	$\epsilon_{max}=0.1$	$\epsilon_{max}=0.5$	$\epsilon_{max}=1$	$\epsilon_{max}=5$	$\epsilon_{max}=10$
The direct problem			0.03	0.03	0.03	0.04	0.15	0.35
The inverse problem, without smoothing	3		1.71	1.72	1.97	2.81	5.50	23.44
	5		0.16	8.29	49.73	53.14		
	8		0.05					
The inverse problem with smoothed boundary conditions	90	3	1.74	1.74	1.76	1.83	3.12	5.57
		5	0.32	4.32	29.54	51.00		
		8	0.35					
	50	3	1.74	1.74	1.75	1.81	2.47	4.55
		5	0.33	1.74	25.54	30.82		
		8	0.35					
	20	3	1.74	1.74	1.74	1.75	2.37	3.62
		5	0.33	1.81	5.33	14.41		
		8	0.38	1.95	6.19	12.98		
	4	3	2.77	2.77	2.76	2.77	2.88	3.50
		5	2.77	2.77	2.76	2.77	2.83	3.00
		8	2.77	2.77	2.77	2.77	2.85	2.79

Table 1. Relative error of temperature distribution at the ring boundary for various disturbances of the boundary conditions with the error ϵ_{max} [%], various f parameters of the SVD algorithm, and various numbers of base functions m for smoothing of boundary conditions.

The inverse matrix $[-B_i \ A_i]^T$ of the inverse problem has been computed with the SVD (singular value decomposition) algorithm with various values of the f parameter [Frackowiak et al. 2006]. Results of calculation of the direct and inverse problems, for example, the distributions of temperature, heat flow density, and surface film conductance at the inner and outer ring boundaries for undisturbed boundary conditions, and the parameter $f = 5$ (with the f parameter affecting only the inverse task), are shown in Figures 8–10.

Moreover, Tables 1 and 2 present relative errors of temperature and heat flow density at the ring boundaries with regard to the analytical solution given by the formula

$$\delta L_{2T} = \frac{\int_{\Gamma} (T - T_{analyt})^2 ds}{\int_{\Gamma} T^2_{analyt} ds} \cdot 100\%, \quad \delta L_{2q} = \frac{\int_{\Gamma} (q - q_{analyt})^2 ds}{\int_{\Gamma} q^2_{analyt} ds} \cdot 100\%. \tag{4-1}$$

The boundary conditions (temperature and heat flow density) in both cases have been disturbed with a relative error given by the formula

$$\epsilon = \epsilon_{max} \cdot (2 \cdot \text{random} - 1), \tag{4-2}$$

Type			Heat flow error δL_{2q} [%]					
	m	f	$\epsilon_{max}=0$	$\epsilon_{max}=0.1$	$\epsilon_{max}=0.5$	$\epsilon_{max}=1$	$\epsilon_{max}=5$	$\epsilon_{max}=10$
The direct problem			0.35	0.35	0.39	0.55	2.42	5.04
The inverse problem, without smoothing	3	18.01	18.04	18.79	21.60	27.68		
	5	3.80						
	8	0.66						
The inverse problem with smoothed boundary conditions	90	3	18.02	18.02	18.08	18.27	22.55	33.28
		5	3.86					
		8	13.47					
	50	3	18.02	18.02	18.05	18.22	20.35	28.91
		5	3.87	34.25				
		8	13.47					
	20	3	18.02	18.02	18.04	18.09	19.47	25.13
		5	3.87	38.05				
		8	13.83	40.52				
	4	3	22.60	22.60	22.61	22.61	23.00	24.88
		5	22.60	22.60	22.60	22.61	22.80	23.55
		8	26.22	26.22	26.22	26.22	26.35	26.26

Table 2. Relative error of heat flow density distribution at the ring boundary for various disturbances of the boundary conditions with the error ϵ_{max} [%], various f parameters of the SVD algorithm, and various numbers of base functions m for smoothing of boundary conditions.

where random is a pseudorandom number in the range (0, 1).

For the inverse problem and disturbed boundary conditions the task has been computed prior to solving it according to the formula (3-2), smoothing temperature and heat flow density at the outer boundary with a trigonometric polynomial [Wróblewska et al. 2008]. The error values (4-1) for various numbers of the trigonometric polynomials used for boundary condition smoothing are shown in Tables 1, 2 and Figures 11, 12.

5. Summary

The FEM method introduced in this paper consists of using base functions φ_i that take zero values at the boundary of the mesh node neighborhood, Figure 2, belonging to the domain Ω . Consequently, the function that approximates the solution of the differential equation in the element is not subject to differentiation.

The method presented in this paper, with disturbed boundary conditions, gave very good values of temperature and flow distributions at the ring boundaries, in the sense of the norm (4-1). In the case of temperature it was below 1%, while for the flow density it was below 14%, with the maximal level of boundary condition disturbance amounting to $\epsilon_{max} = 5\%$.

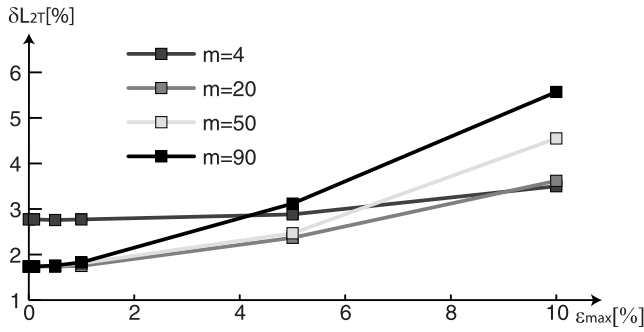


Figure 11. Dependence of relative error of temperature on maximal level of boundary condition disturbance for various numbers of the base functions smoothing the boundary conditions and the parameter $f = 3$.

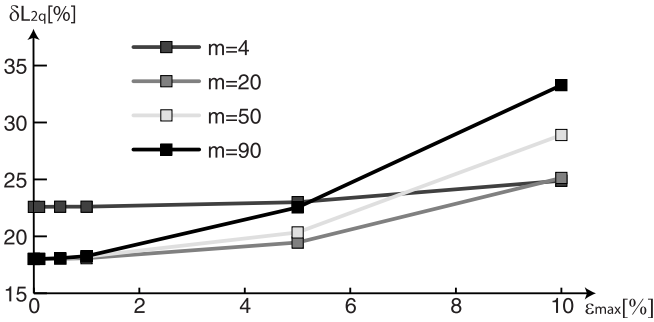


Figure 12. Dependence of relative error of heat flow density on maximal level of boundary condition disturbance for various numbers of the base functions smoothing the boundary conditions and the parameter $f = 3$.

In case of the inverse problem the best results, in the sense of the norm (4-1), have been obtained with the f parameter of the SVD algorithm equal to 3. For temperature it was below 2%, while for the heat flow density below 20%, with a maximal level of temperature and heat flow disturbance at the outer ring boundary amounting to $\epsilon_{max} = 0.5\%$. Smoothing of boundary conditions with the use of linear combination of trigonometric polynomials reduced the error of the norm (4-1). For the flow it dropped below 20% with $\epsilon_{max} = 5\%$ for $f = 3$ and 20 trigonometric functions. In case of higher values of the parameter $f \in (4, 8)$ good results have been achieved only with undisturbed boundary conditions. In case of 4 smoothing functions the error, in the sense of the norm (4-1), remained independent on the parameter f , amounting to less than 3% for the temperature and less than 23% for the flow.

References

[Frąckowiak ≥ 2008] A. Frąckowiak, *Base functions of the Finite Element Method and their properties*, To appear in *Zesz. Nauk. Politech. Poznań*.
 [Frąckowiak et al. 2006] A. Frąckowiak, M. Ciałkowski, and J. von Wolfersdorf, "Numerical solution of a two-dimensional inverse heat transfer problem in gas turbine blade cooling", *Arch. Thermodyn.* **27**:4 (2006), 1–8.

[Gresho and Sani 2000] P. M. Gresho and R. L. Sani, *Incompressible flow and the finite element method*, Wiley, New York, 2000.

[Wróblewska et al. 2008] A. Wróblewska, M. Ciałkowski, and F. A., “Numerical solution of a direct and inverse stationary problem of heat transfer with a modified method of elementary balances”, *Arch. Thermodyn.* **29**:1 (2008), 3–18.

Received 7 Feb 2008. Revised 26 Mar 2008. Accepted 2 Apr 2008.

ANDRZEJ FRĄCKOWIAK: andrzej.frackowiak@put.poznan.pl
Poznań University of Technology, Piotrowo 3, 60-965 Poznań, Poland

JENS VON WOLFERSDORF: jens.vonwolfersdorf@itlr.uni-stuttgart.de
Universität Stuttgart, Institut für Thermodynamik der Luft- und Raumfahrt, Pfaffenwaldring 31, 70569 Stuttgart, Germany

MICHAŁ CIAŁKOWSKI: michal.cialkowski@put.poznan.pl
Poznań University of Technology, Piotrowo 3, 60-965 Poznań, Poland

